HHS Public Access

Author manuscript

J Immunol. Author manuscript; available in PMC 2019 September 15.

Published in final edited form as:

J Immunol. 2018 September 15; 201(6): 1735–1747. doi:10.4049/jimmunol.1800271.

Type 1 interferon and PD-L1 coordinate lymphatic endothelial cell expansion and contraction during an inflammatory immune response

Erin D. Lucas[*,¶], **Jeffrey M. Finlon**[*], **Matthew A. Burchill**[*], **Mary K. McCarthy**[¶], **Thomas E. Morrison**[¶], **Tonya M. Colpitts**[†,#], and **Beth A. Jirón Tamburini**[*,¶]

[*]University of Colorado Anschutz Medical Campus, School of Medicine, Department of Medicine: Division of Gastroenterology and Hepatology, Aurora, CO.

[¶]Department of Immunology and Microbiology, Aurora, CO.

[†]Boston University, National Emerging Infectious Diseases Laboratories, Boston University School of Medicine, Boston, MA.

[#]Department of Microbiology, Boston University School of Medicine, Boston, MA.

Abstract

Lymph node (LN) expansion during an immune response is a complex process that involves the relaxation of the fibroblastic network, germinal center formation, and lymphatic vessel growth. These processes require the stromal cell network of the lymph node to act deliberately in order to accommodate the influx of immune cells to the lymph node. The molecular drivers of these processes are not well understood. Therefore, we asked whether the immediate cytokines, type 1 interferon, produced during viral infection influences the lymphatic network of the lymph node in mice. We found that following an interferon inducing stimulus, such as viral infection or polyI:C, programmed death ligand 1 (PD-L1) expression is dynamically upregulated on lymphatic endothelial cells (LEC). We find that reception of type 1 interferon by LECs is important for the upregulation of PD-L1 of mouse and human LECs and the inhibition of LEC expansion in the LN. Expression of PD-L1 by LECs is also important for the regulation of lymph node expansion and contraction after an interferon inducting stimulus. We demonstrate a direct role for both type 1 interferon and PD-L1 in inhibiting LEC division and in promoting LEC survival. Together these data reveal a novel mechanism for the coordination of type 1 IFN and PD-L1 in manipulating LEC expansion and survival during an inflammatory immune response.

Corresponding Author: Beth A. Jirón Tamburini, Ph.D, Assistant Professor, University of Colorado Anschutz Medical Campus, School of Medicine, Department of Medicine, Division of Gastroenterology and Hepatology, Mail stop B-146, Room P15-10122, 12700 E. 19th Ave., Aurora, CO 80045, beth.tamburini@ucdenver.edu, Phone: 303-724-0182, Fax: 303-724-7243.

Contribution: E.D.L, B.A.J.T., J.M.F., M.K.M. and T.M.C. performed experiments, E.D.L and B.A.J.T. analyzed results and made the figures, E.D.L, B.A.J.T., M.A.B. and T.E.M. designed the research and wrote the paper.

Conflict-of-interest disclosure: The authors declare no competing financial interests.

Introduction

Following either infection or immunization, the draining lymph node (dLN) must expand to accommodate the influx of lymphocytes and then contract as the immune response resolves and the node returns to homeostasis. We and others have demonstrated an increase in both the number of lymphatic endothelial cells (LECs)(1–5) and the density of LECs in the cortical region(6) of the dLN in response to an innate stimulus. Although factors required for lymphatic vessel growth in the tissue have been established and include the VEGFC/VEGFR3 interaction(3–5, 7–11), alternative signaling mechanisms by which the lymphatic endothelium of the lymph node (LN) expand are still not well understood. However, some critical events are required for the expansion of the LN and include the recruitment of B cells, DCs and T cells, prior to expansion and lymphatic remodeling(1, 3–5, 12, 13). Very little is known about the contraction of the LN stroma following an immune response. However, we have demonstrated that the LECs undergo apoptosis during LN contraction(2) and others have noted IFNγ production by T cells results in lymphatic regression during LN contraction(14).

Within the LN, LECs differentially express several markers including programmed cell death ligand 1 (PD-L1), intercellular adhesion molecule 1 (ICAM1), vascular cellular adhesion molecule 1 (VCAM1) and mucosal addressin cellular adhesion molecule (MadCam)(15). Intercellular interactions between LECs and DCs are established by the interaction of ICAM1, VCAM1 and MHC class II on stromal cells; and Lfa1 and Mac-1 on DCs, among others(1, 16–19). These interactions are important for LECs and DCs to interact to exchange antigens and promote either self-tolerance(15, 20, 21) or promote T cell effector memory(1). However, why the LECs express PD-L1 based on their location in the LN (15) is not well understood. The described primary function of PD-L1 expression by the lymphatic endothelium is to drive peripheral T cell tolerance both to self-antigens, non-adjuvanted foreign antigens(15, 17, 20–23) and in settings of cancer(24, 25). It has been demonstrated that PD-L1 expression by cancer cells induces a signaling network that results in increased cellular survival and inhibition of cell division(26–29). However, whether PD-L1 signaling events occur in LECs has yet to be established.

Here, we reveal that PD-L1 expression by LECs in the LN is dynamically regulated during an immune response and that this regulation is dependent on interferon alpha/beta receptor (IFNaR) signaling. Furthermore, we provide evidence that both type 1 IFN and PD-L1 are negative regulators of LEC division during LN expansion. In turn, and in concert with other work(26, 27), we show that PD-L1^{hi} LECs are protected from the apoptotic process that ensues during LN contraction. Therefore, our data outlines a role for type 1 IFN and PD-L1 in regulating the expansion and contraction of the lymphatic network in the LN during an inflammatory immune response.

Methods

Mice.

4–6 week old mice were purchased from Charles River or Jackson Laboratory, unless otherwise stated, bred and housed in the University of Colorado Anschutz Medical Campus

Animal Barrier Facility. Wild type, Prox-1 cre, Rosa26 STOPflox, *Ifnar1*$^{-/-}$, *Ifngr1*$^{-/-}$ and *Pdl1*$^{-/-}$ mice were all bred on a C57BL/6 background. All animal procedures were approved by the Institutional Animal Care and Use Committee at the University of Colorado.

PolyI:C and viral challenge.

PolyI:C (Invivogen) and ovalbumin were injected either subcutaneously or intraperitoneally as described previously(1, 2). For some experiments, anti-CD40 (BioXcell) was also injected. For viral challenge, mice were injected with 1×10^4 pfu/footpad using the vaccinia virus western reserve strain(1, 30). For chikungunya virus infections, 3-4 week-old mice were injected with 10^3 pfu/footpad of the chikungunya virus strain AF15561 or 181/25 in an animal biosafety level 3 laboratory. For Dengue virus infection, 6 week old mice were injected with 10^4 pfu/footpad of the dengue virus strain DENV2 NGC.

BrdU treatment.

4 mg of 5-Bromo-2'-Deoxyuridine (BrdU) (BP25081, Fisher Bioreagents) was injected into C57BL/6 mice in 200 μl of PBS intraperitoneally and given at 0.8 mg/mL BrdU in water for one week(3).

LEC harvesting and staining for flow cytometry.

LNs were harvested and digested, and then stained for flow cytometry(1, 2). For Ki67 staining cells were stained for surface markers and then fixed and permeablized using the eBioscience FoxP3 transcription factor staining buffer set (catalog number 00–523). Briefly, cells were fixed and permeabilized for 30 min at 4°C in the dark, and then stained with Ki67 overnight at 4°C. Cells were then washed and run on the cytometer.

For BrdU studies, cells were stained for surface markers, and then fixed in solution of 4% PFA, 1mg/mL saponin, 1% HEPES in HBSS (PFA/saponin solution) Cells were incubated in 10% DMSO in PBS/saponin buffer on ice for 10min to enhance staining. Cells were re-fixed in PFA/saponin solution for 5min at RT, and then digested with 1mg/mL DNAse for 1 hour. Cells were stained with BRDU FITC (10μL ab into 45μL PBS/saponin buffer) for 30min at 4°C.

For evaluation of caspase activity by flow cytometry, the CellEvent Caspase-3/7 Green Kit (Life Technologies, catalog number C10427) was used. Briefly, cells were digested as described and then stained for surface markers. Cell were then stained with the caspase reagent for 30min at 37°C, and then run on the cytometer.

Unless otherwise noted, all flow cytometry antibodies were purchased from Biolegend. Stromal cells were stained with CD45 APC-Cy7 (1:200) or Pacific Blue (1:300) clone 30-F11, PDPN APC clone 8.1.1 (1:200), CD31 PerCP/Cy5.5 clone clone 390 (1:200), PD-L1 PE or BV421 (1:200) clone 10F.9G2, Ki67 PE clone SolA15 (1:400, eBioscience), BrdU FITC (clone Bu20A, eBioscience or B44, BDBiosciences) and ICAM PE or Pacific Blue clone 3E2 (1:400, BD Pharmingen).

LEC culture.

Primary mLECs (Cell Biologics, C57–6092) and hLECs (Cell Biologics, H-6092) were cultured in in endothelial cell media (Cell biologics, M1168 and H1168). Flasks and plates were coated with matrigel diluted 1:1000 in media(31). mLECS were treated with rIFNα (a kind gift from Ross Kedl(32)) and rIFNγ (Biolegend, 714006) at 250 U/mL(33) for 24 hours (h) before cells were harvested. Cells were then stained with αPDPN and αPD-L1, and acquired on a Cyan ADP flow cytometer (Dako) and analyzed using flowjo software (Treestar). hLECs were treated with human IFNα2 (PBL Assay Science-11100–1) at 500 U/mL(34) for 24 h and then harvested as above.

Fluorescence microscopy.

Popliteal and inguinal LNs from naïve or immunized mice were fixed in formalin and embedded in paraffin. Normal human LNs embedded in paraffin were obtained from the University of Colorado Pathology Core. About 7–10μm sections were cut using a microtome. Slides were baked for two hours at 65°C and then heated in a pressure cooker for 20min in Tris-EDTA pH9 antigen retrieval buffer. Serial sections were stained with lyve-1 (1:400, Abcam polyclonal) and cleaved capsase 3 (1:100, Cell Signaling), or lyve-1 B220-bio (1:100 Biolegend clone RA3–6B2), and PD-L1 (1:50, Biolegend clone 10F.9G2). For sections stained with caspase and lyve-1, sections were first stained for caspase, and then the section was blocked with an α-rabbit IgG, before staining with lyve-1. Secondary antibodies used were anti-rabbit IgG–FITC and anti-rabbit IgG–dylight647 (1:200, Biolegend) anti-rat IgG-dylight647 (Biolegend, 1:100) and streptavidin-PE (Biolegend 1:200). Normal human lymph nodes were purchased, and 7–10μm sections were cut and stained with D2–40 (1:50) and PD-L1 (1:300). Secondary anti-bodies used were anti-mouse IgG-dylight647, and anti-rabbit IgG-FITC. Sections were imaged using a Nikon Eclipse Ti series fluorescent microscope. Images were taken with a Photometrics Coolsnap Dyano fluorescent camera. For image quantification, regions of interest (ROIs) were drawn around the lyve-1 positive regions to designate LECs and the average MFI of PD-L1 expression was taken using the Nikon software. For quantification of cleaved caspase 3, sections were stained with PD-L1 and positive regions identified. A serial section was stained for lyve-1 and cleaved caspase 3. Serial images were overlaid and PD-L1 positive and lyve-1 positive regions were identified as caspase 3 positive or negative and quantified. DAPI staining was used to ensure the cleaved caspase 3 was nuclear. For all images, Lookup Tables (LUTs) were adjusted on each image equally.

LEC sorting and RT-qPCR.

Five C57BL/6 mice per group were immunized. Six days later, mice were euthanized and draining LNs were digested as described above. Cells were stained with CD45-PE (Biolegend) and underwent negative selection using anti-PE microbeads and LS columns (Milltenyi). LECs were sorted on a FACsAria II (BD Biosciences). RNA was isolated from sorted PD-L1^{lo} and PD-L1^{hi} LEC populations with the RNeasy micro kit (Qiagen-74004). Complimentary DNA (cDNA) was made using the Qiagen QuantiTect Reverse Transcription kit (Qiagen-205314). Primers to *Cxcl4, Gdf10, Itgb1* and control gene *18s* were purchased

from Qiagen and run on Thermo Fisher Step 1 plus real-time PCR machine. Quantification was performed using the delta-delta CT method(35).

Bone marrow chimeras.

WT, *Pdl1*$^{-/-}$, or *Ifnar1*$^{-/-}$ were irradiated with 1000 Rads using a Cesium-137 gamma irradiator and rested for 4 h before reconstitution with WT bone marrow. Bone marrow was isolated and red blood cells were lysed prior to intravenous transfer and allowed to reconstitute for 10 weeks(2).

Results:

Dynamic expression of PD-L1 by Lymphatic Endothelial Cells

At homeostasis, subcapsular and medullary mouse LN LECs have been shown to express high levels of PD-L1 while cortical LECs only express low levels(15). Similarly, in normal human LNs stained for the lymphatic vasculature with podoplanin (PDPN) and PD-L1 we found that LECs express PD-L1 in the subcapsular sinus with undetectable staining in the cortex (Fig 1A,B). To determine the signals that regulate this low versus high expression of PD-L1 on LECs, we asked whether primary LECs derived from human (hLEC) lymph nodes have differential expression of PD-L1. We found hLECs at homeostasis do not have low and high PD-L1 expressing populations (Figure 1C). Based on published findings that IFNα could regulate PD-L1 expression in other cell lineages(33, 36–38) we asked if PD-L1 was regulated by IFNα *in vitro*. Upon stimulation with IFNα, PD-L1 expression increased both by surface protein expression (Figure 1C) and mRNA (Figure 1D) in hLECs. Similarly, naïve primary murine LECs (mLECs) express low levels of PD-L1 (Figure 1E), and do not have bimodal expression of PD-L1. Interestingly, upon treatment with polyI:C, pam3CSK or LPS, mLECs did not upregulate PD-L1, but similarly to hLECs, did upregulate PD-L1 in response to recombinant IFNα (Figure 1E, Supplemental Figure 1A) This suggests that LECs are not upregulating PD-L1 in response to the polyI:C, a TLR3 agonist, even though LECs express TLR3 *in vivo* (39), and primary murine LECs express TLR3 *in vitro* (Supplemental Figure 1B). These data demonstrate that type 1 interferon, but not type 1 interferon inducing TLR agonists, is sufficient to cause the upregulation of PD-L1 by LECs.

To address whether PD-L1 expression by LECs changed following type 1 IFN stimulus *in vivo* we evaluated PD-L1 expression by LECs in the lymph nodes of mice. We used Prox-1 ERcre Rosa26 STOPflox Tdtomato mice (prox-1 tdt), which express Tdtomato in prox-1 cre positive cells following tamoxifen administration(40), where prox-1 distinguishes LECs from all other cells in the lymph node(41). We then verified that the prox1 expressing cells were also lyve-1 positive (Figure 1F, Supplemental Figure 1C) and quantified PD-L1 expression. We confirmed PD-L1 staining was not non-specific binding of the anti-rat secondary by staining lymph node sections with the anti-rat secondary alone (Supplemental Figure 1D). While the Tdtomato does appear dimmer in the center of lymph nodes this is likely due to the lack of tamoxifen penetrance.

We quantified PD-L1 expression on LECs in naïve lymph nodes, delineating the subcapsular sinus and the cortex (Supplemental Figure 1C), and confirmed that PD-L1 expression was

higher on subcapsular sinus LECs compared to cortical LECs (Supplemental Figure 1E). The cortical LECs do appear to express PD-L1, but at lower levels than the subcapsular LECs, as has been previously described(15). To test whether PD-L1 expression increased after an interferon inducing stimulus we immunized mice subcutaneously with polyI:C. We found that one day following immunization with polyI:C, there was an increase in PD-L1 expression on the prox-1 tdt, lyve-1 positive vessels of mouse lymph nodes (Figure 1F, Supplemental Figure 1C). Even after immunization the subcapsular LECs expressed higher levels of PD-L1 compared to the cortical LECs (Supplemental Figure 1E). This was not due to differences in IFNaR expression by the LECs as we found no significant differences in IFNaR expression between the PD-L1^{hi} or PD-L1^{lo} LECs (Supplemental Figure 1F).

PD-L1 upregulation by LECs after infection or immunization is controlled by type 1 IFN

To determine if PD-L1 upregulation by LECs *in vivo* is a normal response to viral infection, we infected mice with vaccinia virus, chikungunya virus (CHIKV), and dengue virus and evaluated PD-L1 expression on dLN LECs by immunofluorescence. We first confirmed that in naive mice, PD-L1 expression was lower in the T cell zone and in the interfollicular ridges by visualization of the B cell follicles (Supplemental Figure 2A), but detectable as previously reported(23) and shown (Supplemental Figure 1D). We found a dramatic increase in PD-L1 expression on LECs both in the sinus and in the cortex three to five days after viral infection (Figure 2A, Supplemental Figure 2A). We confirmed these findings using flow cytometry following infection with vaccinia virus, CHIKV or immunization with polyI:C. LECs were gated as CD45^{-}, CD31^{+}, PDPN^{+}, and then PD-L1 expression was examined (Supplemental Figure 2B). Following infection or immunization with polyI:C, PD-L1 expression on LECs increased significantly (~5 fold) compared with LECs in naive mice (Figure 2B). To understand the kinetics of PD-L1 upregulation we immunized mice and evaluated PD-L1 expression over time. We found that PD-L1 upregulation occurred within 3 hours post immunization with polyI:C, where the peak of expression occurred at 24 hours (Figure 2C,D). PD-L1 expression returned to steady-state levels between day 3 and 6 after polyI:C immunization (Figure 2D).

Importantly, dengue virus, polyI:C, vaccinia virus, and CHIKV are all potent inducers of type 1 IFN(42–45), which is capable of inducing PD-L1 expression on both human and murine LECs *in vitro* (Figure 1). While administration of TLR agonists *in vitro* was not sufficient to induce the upregulation of PD-L1, immunization with other type 1 IFN inducing TLR agonists LPS and CpG did result in the upregulation of PD-L1 on LECs *in vivo*. However, immunization with Pam3CSK, a TLR1,2 agonist that does not induce type 1 IFN, did not lead to PD-L1 upregulation (Supplemental Figure 2C). Indeed, we found a dramatic increase in IFNβ expression and an increase in IFNα4 expression in the LN at 5 hours which decreased, but was still high, at 1 day post immunization by qRT-PCR (Figure 2E) after polyI:C immunization. We also evaluated IFNγ expression, as Type 2 IFNs have also been shown to upregulate PD-L1(33, 36, 46–49), and found that IFNγ expression does increase in the lymph node at 5 hours post polyI:C immunization, but not to the extent of IFNα4 and IFNβ and decreased by day 1. There was no detectable expression of IFNα4, IFNβ or IFNγ at 3 or 4 days after immunization (Figure 2E) when PD-L1 expression also returns to normal levels (Figure 2D). Following this immunization, we know that IFNγ is

produced by T cells by day 6(50) and that this does not result in PD-L1 upregulation (Figure 2D). To determine if type 1 IFN is required *in vivo* for PD-L1 upregulation by LECs in the LN, we utilized mice deficient in interferon alpha/beta receptor 1 (*Ifnar1*$^{-/-}$). WT and *Ifnar*$^{-/-}$ mice were immunized with polyI:C and one day after immunization PD-L1 expression by LN LECs was evaluated. While PD-L1 expression increased on WT LECs, the LECs from *Ifnar*$^{-/-}$ mice did not upregulate PD-L1 expression in response to immunization (Figure 2F).

To determine the role of type 1 IFN in regulating PD-L1 on LECs following infection we infected *Ifnar*$^{-/-}$ mice with vaccinia virus and evaluated PD-L1 expression on LECs five days post infection. Intriguingly, PD-L1 expression in the *Ifnar*$^{-/-}$ hosts was not as high as in WT mice infected with vaccinia virus (Figure 2F), perhaps indicating that there are other factors produced during viral infection that lead to the partial upregulation of PD-L1 on LECs. However, there was a significant decrease in PD-L1 expression following both polyI:C and vaccinia in the *Ifnar*$^{-/-}$ hosts (Figure 2G). PD-L1 expression in the naïve *Ifnar*$^{-/-}$ host was similar to the WT naïve, indicating that type 1 IFNs are not necessary for the homeostatic bimodal expression of PD-L1 on LECs *in vivo*, which is consistent with published data suggesting that lymphotoxin beta receptor (Ltβr) expression may be necessary for steady state PD-L1 expression in the LN(15). These data demonstrate that type 1 IFNs are critical for the upregulation of PD-L1 on LECs at early time-points following both immunization and infection. Since IFNγ treatment can induce PD-L1 expression by LEC (Supplemental figure 2D) and other endothelial cells *in vitro*(33, 36, 46–49) we asked if IFNγ was also responsible for the upregulation of PD-L1 *in vivo* following immunization. One day post immunization, in IFNγ deficient mice, PD-L1 expression on LECs increased despite the inability of LECs to receive a signal from IFNγ (Supplemental Figure 2E) indicating that IFNγ is not required for PD-L1 upregulation in response to polyI:C *in vivo* but is sufficient *in vitro*. Collectively, these data indicate that PD-L1 expression on LN LECs *in vivo* is regulated by IFNaR signaling following both polyI:C immunization and viral infection.

PD-L1^{lo} LECs divide during LN expansion

The timing in which PD-L1 expression occurs, 0–3 days (Figure 2D), is prior to the expansion of LECs (3–6 days)(1) after immunization (Figure 3A). Therefore, we asked if there was a connection between PD-L1 expression and LEC division. Mice were immunized as above with antigen (ovalbumin) and polyI:C with or without αCD40 to elicit LN expansion and LEC division (Figure 3A and Supplemental Figure 3A). To our surprise, by Ki67 staining, only the PD-L1^{lo} LECs underwent division at 3–6 days post immunization (Figure 3A) concurrent with the time-point in which PD-L1 expression declined (Figure 2D). This difference in division between the PD-L1^{lo} and the PD-L1^{hi} LECs was reflected in the number of LECs over the course of the immune response (Figure 3B). Although there was a dramatic increase in the number and frequency of PD-L1^{hi} LECs at one day post immunization, corresponding with the overall increase in PD-L1 expression, the PD-L1^{hi} LEC subset did not divide during LN expansion (3–6 days), whereas the PD-L1^{lo} LEC subset significantly expanded in the days following immunization (Figure 3B). These data

demonstrate that PD-L1 expression negatively correlates with the expansion of LECs in response to type 1 IFN inducing innate stimuli.

To investigate how LEC division is controlled following an innate immune stimulus and whether these two populations of LECs, PD-L1^{hi} versus PD-L1^{lo}, activate different transcriptional programs, we immunized mice with polyI:C and evaluated the known growth factor receptor associated with LEC division, vascular endothelial cell growth factor receptor 3 (VegfR3). Following repeated systemic injection of the blocking VEGFR3 antibody we did not observe any difference LEC proliferation after immunization, as assessed by Ki67 staining of LN LECs between 1 day and 7 days post immunization (Supplemental Figure 3B). Therefore, we analyzed expression of other factors known to be involved in endothelial growth or inhibition of growth. To do this we digested the LN and sorted LECs (1, 2, 51), based on their expression of PD-L1 (Supplemental Figure 3C,D) 5 days after immunization- a timepoint when we saw robust LEC division. We did not observe any difference in VEGFR3/Flt4 expression between PD-L1^{hi} and PD-L1^{lo} LECs (Figure 3C). We evaluated the angiostatin platelet factor 4 (PF4/CXCL4) shown to be important in inhibiting angiogenesis (52, 53) by binding to vascular growth factor receptors(54) and found an approximately 50 fold increase of PF4/CXCL4 expression in PD-L1^{hi} LECs (Figure 3C). We also evaluated growth/differentiation factor 10 (GDF10) which was shown to be involved in the growth of CD31^{+} endothelial cells as well as axonal sprouting(55). GDF10 was enriched 50–100 fold in the PD-L1^{lo} LECs (Figure 3C). Finally, we evaluated integrin β 1 (ITGB1) expression due to its involvement in endothelial growth and sprouting(56, 57), and found ITGB1 was enriched in the PD-L1^{lo} LECs approximately 2–6 fold (Figure 3C). Together, these data suggest that PD-L1^{lo} LECs have a transcriptional program associated with active cell division while PD-L1^{hi} LECs actively inhibit cell division.

Early LEC division is inhibited by type 1 IFN

Due to the dramatic differences in division we found between PD-L1^{hi} and PD-L1^{lo} LECs in the LN, the delay in LEC division between days 0 and 3 (Figure 3A,B) and the kinetics of IFN expression in the LN after polyI:C immunization (Figure 2E) we asked if type 1 IFNs were inhibiting LEC division. Using a lethally irradiated *Ifnar*$^{-/-}$ mouse reconstituted with WT bone marrow we asked again whether the LECs upregulated PD-L1 after polyI:C immunization (Figure 4A). We found the LECs lacking the IFNaR, even when the hematopoietic compartment was WT, could not upregulate PD-L1 (Figure 4B,C). Surprisingly, we saw robust division in the *Ifnar*$^{-/-}$ host two days following immunization (Figure 4B,D), with around 20% of the LECs dividing, in contrast to the WT mice where very little division (around 5%) occurred at 2 days post immunization (Figure 4D and Supplemental Figure 3A). As before, only the PD-L1^{lo} LECs divided following immunization suggesting that PD-L1^{lo} LEC preference for division is not controlled by type 1 IFN signaling. To determine if chronic IFN signaling results in loss of LEC division we utilized a chronic polyI:C injection model(58) (Figure 4E). Based on the data above we predicted that chronic IFN signaling would result in sustained upregulation of PD-L1 in the LN. Indeed, when mice were injected with polyI:C every other day for 1 week, PD-L1 expression remained high over the course of the week while a single injection of polyI:C resulted in the downregulation of PD-L1 at 4 days following immunization (Figure 4F).

When we evaluated the expression of Ki67 by LECs we again found that Ki67 was produced at high levels at 4 days following a single injection of polyI:C, concurrent with the time-point in which PD-L1 expression decreased. Consistent with the loss of type 1 IFN signaling inducing dysregulated division in the *Ifnar*$^{-/-}$ chimera (Figure 4a-c), we found that chronic type 1 IFN signaling significantly inhibited the ability of the cells to divide (Figure 4G). Taken together, we conclude that type 1 IFN, resulting from an innate stimulus, inhibits LEC division during the time when IFNα and IFNβ expression is elevated (Figure 2E).

Loss of PD-L1 increases LEC division

We have shown above that PD-L1 distinguishes which LECs will divide during lymph node expansion, however it has been shown that high levels of PD-L1 can inhibit vascular endothelial cell division through vascular endothelial cell growth factor regulation *in vitro*(28). Since we see selective division of PD-L1^{lo} LECs after IFN expression declines, we asked if PD-L1 was also contributing to the control of LEC division. We first asked if complete loss of PD-L1 led to aberrant LEC division. We utilized *Pdl1*$^{-/-}$ mice to determine if LEC division after immunization was affected when PD-L1 was absent. We used both total *Pdl1*$^{-/-}$ mice and *Pdl1*$^{-/-}$ mice lethally irradiated and reconstituted with WT bone marrow to eliminate any contribution of PD-L1 coming from hematopoietic cells such as macrophages and DCs. We found that there was significantly more LEC division in the total *Pdl1*$^{-/-}$ host and in the chimeric *Pdl1*$^{-/-}$ host compared to each WT counterpart at 5 days post immunization (Figure 5A). This increase in division corresponded with a greater fold increase in total LEC number in the *Pdl1*$^{-/-}$ host than the WT host independent of whether it was a complete *Pdl1*$^{-/-}$ or bone marrow chimera (Figure 5B). When we asked if loss of PD-L1 could initiate LEC division earlier we found that, unlike the *Ifnar*$^{-/-}$ chimeras, in the *Pdl1*$^{-/-}$ chimera there was no increase in LEC division at 2 days post immunization (Figure 5A), nor an increase in division in the *Pdl1*$^{-/-}$ mice during chronic polyI:C immunization (Supplemental Figure 4B), indicating that the role of PD-L1 in regulating division is independent and secondary to type 1 IFN. Importantly, we did not observe any differences in total LN cell number, CD4 and CD8 T cell number or B cell number between the WT and the *Pdl1*$^{-/-}$ host or *Pdl1*$^{-/-}$ chimera (Supplemental Figure 4C), indicating that the differences observed in LEC division or number was not simply due to increased LN size or cellularity.

To evaluate whether LEC division was dysregulated in the population of LECs that normally express PD-L1, we used ICAM1 as a marker of subcapsular LECs, as described previously (15 and Supplemental figure 2B). The expression of ICAM1 does not change in the *Pdl1*$^{-/-}$ chimera compared to WT (Figure 5C). We found that in the WT type hosts, very few of the ICAM1^{+} LECs divided during LN expansion; strikingly, a substantial number of ICAM1^{+} LECs underwent division in the *Pdl1*$^{-/-}$ chimera (Figure 5C,D). We then evaluated whether there were differences in the factors involved in endothelial growth and/or inhibition we had seen between PD-L1^{hi} and PD-L1^{lo} LECs in the *Pdl1*$^{-/-}$ mice. Thus, we immunized mice and 5 days later digested the LNs and sorted LECs. While we found no significant differences in either GDF10 or ITGB we saw decreased expression of the angiostatin, CXCL4 (Figure 5E). As CXCL4 has been shown to negatively regulate angiogenesis (52–54), a reduction in CXCL4 expression may be one mechanism by which LEC division increases in the *Pdl1*$^{-/-}$ chimeras. These data demonstrate a role for PD-L1 in regulating

LEC growth, perhaps through the inhibition of CXCL4, during the process of LN expansion after an immune stimulus.

PD-L1^{lo} LECs undergo apoptosis during lymph node contraction

Other reports outline a role for PD-L1 in promoting cancer cell survival (26, 27, 29), via domains in the cytoplasmic tail of PD-L1(26, 29). Our previous findings suggest that LEC apoptosis occurs during LN contraction (2). Thus, we asked whether PD-L1 expression was promoting LEC survival of specific subsets of LECs. Therefore, we utilized a pulse-chase experiment where immediately following immunization with polyI:C and αCD40, BrdU was given to mice for one week to allow the BrdU to incorporate into DNA during DNA replication (Figure 6A). After one week of BrdU, mice were given normal water for two more weeks to evaluate the loss of cells that incorporated BrdU and thus which cells underwent LEC death (Figure 6A). At one-week post immunization, we observed BrdU incorporation in the PD-L1^{lo} LECs, but not in the PD-L1^{hi} LECs, confirming our Ki67 results that PD-L1 expressing LECs do not undergo division (Figure 6B). To evaluate which populations underwent contraction we evaluated the loss of BrdU+ or BrdU- cells. When we quantified the number of PD-L1^{lo} LECs between 1 week and 3 weeks we found a significant loss in PD-L1^{lo} BrdU+ LECs (Figure 6C), while we saw similar numbers of PD-L1^{hi} LECs between week 1 and week 3 (Figure 6D). These data suggest that not only do the PD-L1^{lo} LECs divide in response to an immune stimulus, but that they are also the cells that contract during the resolution of the immune response.

To directly determine if low PD-L1 expression marks LECs that undergo caspase mediated apoptosis during LN contraction we immunized mice and 2 weeks later asked which LECs expressed caspase3/7 using caspase flow reagent (Figure 6E). Consistent with the above data (Figure 6C,D), PD-L1 expression inversely correlated with the expression of caspase 3/7 by LECs (Figure 6E,F). We also evaluated explanted LNs from mice immunized 10 days prior to evaluate caspase staining by immunofluorescence. We stained serial sections with lyve-1 and cleaved caspase 3, or PD-L1 and quantified the number of caspase 3+ cells that were either lyve-1+PD-L1^{hi} or lyve-1+PD-L1^{lo} (Yellow arrows, Figure 6G). To ensure we only evaluated caspase 3^{+} LECs, only cells where caspase 3 overlapped with DAPI, in lyve-1^{+} vessels were counted. Further, we used sections stained without the primary caspase antibody to distinguish caspase staining from non-specific staining (Supplemental Figure 4A). White arrows indicate caspase 3+ cells that are not lyve-1 positive. The number of caspase positive PD-L1^{lo} LECs per LN was significantly higher than the number of caspase positive PD-L1^{hi} LECs, indicating that PD-L1^{lo} LECs undergo apoptosis at a higher frequency than PD-L1^{hi} LECs. Together, these data demonstrate that, during an acute, inflammatory immune response, the PD-L1^{lo} LECs divide and then undergo apoptosis during LN expansion and contraction, respectively, while the PD-L1^{hi} LECs neither divide nor die during an immune response.

PD-L1 protects LECs from apoptosis

We next asked if loss of PD-L1 increased LEC apoptosis during an immune response at times other than LN contraction, as we saw only a low frequency of PD-L1 expressing LECs that underwent apoptosis during LN contraction. To address this, we immunized WT mice

and 5 days after immunization, we evaluated caspase 3/7 positive LECs (Figure 7A). Following our normal digestion and staining protocol we observed approximately 40 percent of LECs were caspase 3/7 positive with the majority being PD-L1^{lo} (~30%) (Figure 7B). To evaluate if PD-L1 was acting to protect LECs from death we performed the same procedure in *Pdl1*$^{-/-}$ mice and found a higher mean fluorescence intensity of caspase 3/7 in the *Pdl1*$^{-/-}$ LECs (Figure 7C) indicating the level of caspase 3/7 activity per cell is higher in LECs when PD-L1 is absent. Remarkably, we found a significant increase the percent (Figure 7D) and number (Figure 7E) of caspase positive LECs in the *Pdl1*$^{-/-}$ mice compared to WT mice, indicating that PD-L1 is protective against apoptosis. This is consistent with published data demonstrating a pro-survival effect of PD-L1 signaling in tumor cells (26, 27, 29). These data support the conclusion that there are distinct populations of LECs in the LN that undergo division, apoptosis and survival during LN expansion and contraction. Thus, we propose a model where type 1 IFN and PD-L1 independently inhibit LEC division and where PD-L1 expression promotes LEC survival (Figure 7F).

Discussion

The data presented here support a model where PD-L1 expression by LN LECs regulates the expansion, contraction and survival of LECs in the LN. Some of the factors needed for LEC expansion in the LN during an immune response have be identified, and include production of VEGF-C, as well as DC, T cell and B cell recruitment(4, 5). We find that PD-L1 expression not only regulates LEC division and survival, but that PD-L1 is dynamically regulated by type 1 IFN. Furthermore, we find that type 1 IFN signaling also regulates LEC division in a pathway independent of PD-L1. Our data uncover a novel mechanism by which PD-L1 drives LEC survival and inhibits LEC division explaining the described phenomenon of specific cortical LEC expansion following an immune stimulus(6).Thus, PD-L1 expression by LECs is intertwined with the innate immune response following an immune challenge. Inhibition of LEC division and PD-L1 regulation by type 1 IFN may be a critical first signal for the LECs to pause, perhaps allowing for the relaxation and spreading of the fibroblastic reticular cell network (FRC), which also requires DC-FRC interactions(13), before initiating lymphatic expansion to draw in large numbers of tissue resident immune cells. The immediate upregulation of PD-L1 may be important for preventing an active immune response against self-antigens or non-adjuvanted antigens normally presented by LECs to T cells to maintain peripheral tolerance(15, 17, 20, 21, 25, 59).

We provide ample evidence here that both loss of PD-L1 and IFNaR results in increased LEC division both in a *Pdl1*$^{-/-}$ chimeric mouse model, the intact *Pdl1*$^{-/-}$ mouse and in an *Ifnar*$^{-/-}$ chimeric mouse (Figure 4,5). We also suggest that PD-L1 signaling may lead to downstream CXCL4 activation as CXCL4 expression is decreased in the *Pdl1*$^{-/-}$ mice. Since CXCL4 has been shown to inhibit EC division we predict that loss of CXCL4 results, at least in part, in the increased LEC division we see in the *Pdl1*$^{-/-}$. These data are intriguing as others have shown that CXCL4 is also involved in neutrophil recruitment during inflammation(60) and that neutrophils contribute to inflammatory lymphangiogenesis through VEGFD(61). While GDF10 and ITGB1 are not changed in the *Pdl1*$^{-/-}$ they may still be important for differences between PD-L1^{hi} and PD-L1^{lo} LECs in the WT mouse. We further show that repeated polyI:C injection and chronic interferon results in maintained

upregulation of PD-L1 and in a loss of LEC division at the 3–4 day timepoint during which we and others have described LEC division to occur(1, 4, 5). This loss of LEC division may occur as a result of IFN mediated inhibition or increased PD-L1 inhibition, or both. Interestingly, the loss of LEC division during chronic polyI:C injection never recovers. Not only do these data predict that interferon stimulation and PD-L1 upregulation inhibit LEC division, but also that chronic interferon signaling is likely to have detrimental effects to the normal immune response. This is borne out in the literature in models where chronic interferon signaling dramatically reduces immunity and promotes increased PD-1 expression by T cells and PD-L1 expression by DCs(62–71). We acknowledge that there are likely other cells participating in the process of immune dysregulation during chronic interferon signaling, however, it does appear that in addition to these other cell types, LEC proliferation during LN expansion does not occur normally in situations of chronic interferon stimulation.

Finally, we found that high levels of PD-L1 expression protected LECs from undergoing apoptosis regardless of the timing after immunization. These data indicate that that PD-L1 expression also promotes LEC survival consistent with a described phenomenon in cancer cells(26, 27, 29), where it appears that there are signaling motifs in the C-terminal cytoplasmic domain of PD-L1 that confer protection against multiple inducers of apoptosis(27, 29). The findings we outline here are important as they demonstrate that reverse signaling of PD-L1 is not an aberrant process that occurs only in mutated cancer cells, but instead a process that regulates how the lymph node expands and contracts in response to immunization or infection. With this in mind, we predict that these findings and future studies may provide an understanding of consequences resulting from the inhibition or promotion of PD-L1 reverse signaling in settings of cancer or chronic infection. This is important as we provide evidence that PD-L1 expression and regulation by type 1 IFN also occurs in normal human LNs and primary human LECs (Figure 1).

The role of PD-1 and CD80 expression by hematopoietic cells in PD-L1 reverse signaling also needs to be considered. Current literature suggests that the survival benefit of PD-L1 expression may be independent of binding to PD-1 or CD80, as cells that express PD-L1 survive better in cultures even in the absence of cells expressing PD-1 or CD80(26, 27, 29). However, it is still unclear whether CD80 or PD-1 may contribute. As such, an *in vitro* study with vascular endothelial cells found that PD-L1 expression could limit vascular endothelial cell division and that suppression of CD80 increased VEGFR2 expression thereby promoting division (28).

In summary, these studies outline a role for PD-L1 in regulating the LEC response to an immune stimulus. We have identified a major role for type 1 IFN in the upregulation of PD-L1 on LECs and in the inhibition of LEC division when IFNαβ expression is high. These data corroborate new findings that type 1 IFN can inhibit lymphatic growth during infection(72). We also identified a novel role for PD-L1 reverse signaling into the LEC that prevents LEC expansion after infection or immunization. We show that loss of PD-L1 results in lymphatic expansion after IFN levels decrease in the LN, potentially so that tissue resident cells can infiltrate the LN when it is primed to do so. Finally, we provide evidence that PD-L1 expression leads to an LEC state that confers protection against apoptosis and inhibits division. Taken together these studies identify a novel role for IFNα and PD-L1 in regulating

LEC division during the initiation of the immune response. Future studies are aimed at evaluating the downstream mechanisms by which PD-L1 signals into the LEC, as well as a role for PD-L1^{hi} LECs in coordinating the immune response via interactions with migratory dendritic cells as they enter the lymph node.

Supplementary Material

Refer to Web version on PubMed Central for supplementary material.

Acknowledgements:

We would like to thank Dr. Dong (Mayo Clinic, Rochester MN) for the *Pdl1*$^{-/-}$ mice, Dr. Lenz (University of Colorado AMC) for the *Ifngr*$^{-/-}$ and *Ifnar*$^{-/-}$ mice, and Dr. Kedl (University of Colorado AMC) for the recombinant mouse IFNα.

Funding

This work was supported by a grant from the National Institutes of Health (R01 AI121209)(B.A.J.T.) and the National Institutes of Health T32 AI007405 “Training in Immunology” (E.D.L).

References:

1. Tamburini BA, Burchill MA, and Kedl RM. 2014 Antigen capture and archiving by lymphatic endothelial cells following vaccination or viral infection. Nat Commun 5: 3989. [PubMed: 24905362]
2. Kedl RM, Lindsay RS, Finlon JM, Lucas ED, Friedman RS, and Tamburini BAJ. 2017 Migratory dendritic cells acquire and present lymphatic endothelial cell-archived antigens during lymph node contraction. Nat Commun 8: 2034. [PubMed: 29229919]
3. Webster B, Ekland EH, Agle LM, Chyou S, Ruggieri R, and Lu TT. 2006 Regulation of lymph node vascular growth by dendritic cells. J Exp Med 203: 1903–1913. [PubMed: 16831898]
4. Chyou S, Benahmed F, Chen J, Kumar V, Tian S, Lipp M, and Lu TT. 2011 Coordinated regulation of lymph node vascular-stromal growth first by CD11c+ cells and then by T and B cells. J Immunol 187: 5558–5567. [PubMed: 22031764]
5. Angeli V, Ginhoux F, Llodra J, Quemeneur L, Frenette PS, Skobe M, Jessberger R, Merad M, and Randolph GJ. 2006 B cell-driven lymphangiogenesis in inflamed lymph nodes enhances dendritic cell mobilization. Immunity 24: 203–215. [PubMed: 16473832]
6. Tan KW, Yeo KP, Wong FH, Lim HY, Khoo KL, Abastado JP, and Angeli V. 2012 Expansion of cortical and medullary sinuses restrains lymph node hypertrophy during prolonged inflammation. J Immunol 188: 4065–4080. [PubMed: 22430738]
7. Kaipainen A, Korhonen J, Mustonen T, van Hinsbergh VW, Fang GH, Dumont D, Breitman M, and Alitalo K. 1995 Expression of the fms-like tyrosine kinase 4 gene becomes restricted to lymphatic endothelium during development. Proc Natl Acad Sci U S A 92: 3566–3570. [PubMed: 7724599]
8. Enholm B, Jussila L, Karkkainen M, and Alitalo K. 1998 Vascular endothelial growth factor-C: A growth factor for lymphatic and blood vascular endothelial cells. Trends in Cardiovascular Medicine 8: 292–297. [PubMed: 14987553]
9. Lymboussaki A, Partanen TA, Olofsson B, Thomas-Crusells J, Fletcher CDM, de Waal RMW, Kaipainen A, and Alitalo K. 1998 Expression of the Vascular Endothelial Growth Factor C Receptor VEGFR-3 in Lymphatic Endothelium of the Skin and in Vascular Tumors. The American Journal of Pathology 153: 395–403. [PubMed: 9708800]
10. Rutkowski JM, Ihm JE, Lee ST, Kilarski WW, Greenwood VI, Pasquier MC, Quazzola A, Trono D, Hubbell JA, and Swartz MA. 2013 VEGFR-3 neutralization inhibits ovarian lymphangiogenesis, follicle maturation, and murine pregnancy. Am J Pathol 183: 1596–1607. [PubMed: 24036251]

11. Guc E, Briquez PS, Foretay D, Fankhauser MA, Hubbell JA, Kilarski WW, and Swartz MA. 2017 Local induction of lymphangiogenesis with engineered fibrin-binding VEGF-C promotes wound healing by increasing immune cell trafficking and matrix remodeling. Biomaterials 131: 160–175. [PubMed: 28410495]
12. Acton SE, Farrugia AJ, Astarita JL, Mourao-Sa D, Jenkins RP, Nye E, Hooper S, van Blijswijk J, Rogers NC, Snelgrove KJ, Rosewell I, Moita LF, Stamp G, Turley SJ, Sahai E, and Reis e Sousa C. 2014 Dendritic cells control fibroblastic reticular network tension and lymph node expansion. Nature 514: 498–502. [PubMed: 25341788]
13. Astarita JL, Cremasco V, Fu J, Darnell MC, Peck JR, Nieves-Bonilla JM, Song K, Kondo Y, Woodruff MC, Gogineni A, Onder L, Ludewig B, Weimer RM, Carroll MC, Mooney DJ, Xia L, and Turley SJ. 2015 The CLEC-2-podoplanin axis controls the contractility of fibroblastic reticular cells and lymph node microarchitecture. Nat Immunol 16: 75–84. [PubMed: 25347465]
14. Kataru RP, Kim H, Jang C, Choi DK, Koh BI, Kim M, Gollamudi S, Kim YK, Lee SH, and Koh GY. 2011 T lymphocytes negatively regulate lymph node lymphatic vessel formation. Immunity 34: 96–107. [PubMed: 21256057]
15. Cohen JN, Tewalt EF, Rouhani SJ, Buonomo EL, Bruce AN, Xu X, Bekiranov S, Fu YX, and Engelhard VH. 2014 Tolerogenic properties of lymphatic endothelial cells are controlled by the lymph node microenvironment. PLoS One 9: e87740. [PubMed: 24503860]
16. Podgrabinska S, Kamalu O, Mayer L, Shimaoka M, Snoeck H, Randolph GJ, and Skobe M. 2009 Inflamed lymphatic endothelium suppresses dendritic cell maturation and function via Mac-1/ICAM-1-dependent mechanism. J Immunol 183: 1767–1779. [PubMed: 19587009]
17. Rouhani SJ, Eccles JD, Riccardi P, Peske JD, Tewalt EF, Cohen JN, Liblau R, Makinen T, and Engelhard VH. 2015 Roles of lymphatic endothelial cells expressing peripheral tissue antigens in CD4 T-cell tolerance induction. Nat Commun 6: 6771. [PubMed: 25857745]
18. Teijeira A, Rouzaut A, and Melero I. 2013 Initial afferent lymphatic vessels controlling outbound leukocyte traffic from skin to lymph nodes. Front Immunol 4: 433. [PubMed: 24368908]
19. Petrova TV, and Koh GY. 2018 Organ-specific lymphatic vasculature: From development to pathophysiology. J Exp Med 215: 35–49. [PubMed: 29242199]
20. Cohen JN, Guidi CJ, Tewalt EF, Qiao H, Rouhani SJ, Ruddell A, Farr AG, Tung KS, and Engelhard VH. 2010 Lymph node-resident lymphatic endothelial cells mediate peripheral tolerance via Aire-independent direct antigen presentation. J Exp Med 207: 681–688. [PubMed: 20308365]
21. Dubrot J, Duraes FV, Potin L, Capotosti F, Brighouse D, Suter T, LeibundGut-Landmann S, Garbi N, Reith W, Swartz MA, and Hugues S. 2014 Lymph node stromal cells acquire peptide-MHCII complexes from dendritic cells and induce antigen-specific CD4(+) T cell tolerance. J Exp Med 211: 1153–1166. [PubMed: 24842370]
22. Baptista AP, Roozendaal R, Reijmers RM, Koning JJ, Unger WW, Greuter M, Keuning ED, Molenaar R, Goverse G, Sneeboer MM, den Haan JM, Boes M, and Mebius RE. 2014 Lymph node stromal cells constrain immunity via MHC class II self-antigen presentation. Elife 3.
23. Hirosue S, Vokali E, Raghavan VR, Rincon-Restrepo M, Lund AW, Corthesy-Henrioud P, Capotosti F, Halin Winter C, Hugues S, and Swartz MA. 2014 Steady-state antigen scavenging, cross-presentation, and CD8+ T cell priming: a new role for lymphatic endothelial cells. J Immunol 192: 5002–5011. [PubMed: 24795456]
24. Dieterich LC, Ikenberg K, Cetintas T, Kapaklikaya K, Hutmacher C, and Detmar M. 2017 Tumor-Associated Lymphatic Vessels Upregulate PDL1 to Inhibit T-Cell Activation. Front Immunol 8: 66. [PubMed: 28217128]
25. Lund AW, Duraes FV, Hirosue S, Raghavan VR, Nembrini C, Thomas SN, Issa A, Hugues S, and Swartz MA. 2012 VEGF-C promotes immune tolerance in B16 melanomas and cross-presentation of tumor antigen by lymph node lymphatics. Cell Rep 1: 191–199. [PubMed: 22832193]
26. Ghebeh H, Lehe C, Barhoush E, Al-Romaih K, Tulbah A, Al-Alwan M, Hendrayani SF, Manogaran P, Alaiya A, Al-Tweigeri T, Aboussekhra A, and Dermime S. 2010 Doxorubicin downregulates cell surface B7-H1 expression and upregulates its nuclear expression in breast cancer cells: role of B7-H1 as an anti-apoptotic molecule. Breast Cancer Research 12.

27. Azuma T, Yao S, Zhu G, Flies AS, Flies SJ, and Chen L. 2008 B7-H1 is a ubiquitous antiapoptotic receptor on cancer cells. Blood 111: 3635–3643. [PubMed: 18223165]
28. Jin Y, Chauhan SK, El Annan J, Sage PT, Sharpe AH, and Dana R. 2011 A novel function for programmed death ligand-1 regulation of angiogenesis. Am J Pathol 178: 1922–1929. [PubMed: 21435468]
29. Gato-Canas M, Zuazo M, Arasanz H, Ibanez-Vea M, Lorenzo L, Fernandez-Hinojal G, Vera R, Smerdou C, Martisova E, Arozarena I, Wellbrock C, Llopiz D, Ruiz M, Sarobe P, Breckpot K, Kochan G, and Escors D. 2017 PDL1 Signals through Conserved Sequence Motifs to Overcome Interferon-Mediated Cytotoxicity. Cell Rep 20: 1818–1829. [PubMed: 28834746]
30. Norbury CC, Malide D, Gibbs JS, Bennink JR, and Yewdell JW. 2002 Visualizing priming of virus-specific CD8+ T cells by infected dendritic cells in vivo. Nat Immunol 3: 265–271. [PubMed: 11828323]
31. Lyons TR, Borges VF, Betts CB, Guo Q, Kapoor P, Martinson HA, Jindal S, and Schedin P. 2014 Cyclooxygenase-2-dependent lymphangiogenesis promotes nodal metastasis of postpartum breast cancer. J Clin Invest 124: 3901–3912. [PubMed: 25133426]
32. McWilliams JA, Sanchez PJ, Haluszczak C, Gapin L, and Kedl RM. 2010 Multiple innate signaling pathways cooperate with CD40 to induce potent, CD70-dependent cellular immunity. Vaccine 28: 1468–1476. [PubMed: 19995538]
33. Muhlbauer M, Fleck M, Schutz C, Weiss T, Froh M, Blank C, Scholmerich J, and Hellerbrand C. 2006 PD-L1 is induced in hepatocytes by viral infection and by interferon-alpha and -gamma and mediates T cell apoptosis. J Hepatol 45: 520–528. [PubMed: 16876901]
34. Sharara AI, Perkins DJ, Misukonis MA, Chan SU, Dominitz JA, and Weinberg JB. 1997 Interferon (IFN)-alpha activation of human blood mononuclear cells in vitro and in vivo for nitric oxide synthase (NOS) type 2 mRNA and protein expression: possible relationship of induced NOS2 to the anti-hepatitis C effects of IFN-alpha in vivo. J Exp Med 186: 1495–1502. [PubMed: 9348307]
35. Livak KJ, and Schmittgen TD. 2001 Analysis of relative gene expression data using real-time quantitative PCR and the 2(-Delta Delta C(T)) Method. Methods 25: 402–408. [PubMed: 11846609]
36. Eppihimer MJ, Gunn J, Freeman GJ, Greenfield EA, Chernova T, Erickson J, and Leonard JP. 2002 Expression and regulation of the PD-L1 immunoinhibitory molecule on microvascular endothelial cells. Microcirculation 9: 133–145. [PubMed: 11932780]
37. Schreiner B, Mitsdoerffer M, Kieseier BC, Chen L, Hartung HP, Weller M, and Wiendl H. 2004 Interferon-beta enhances monocyte and dendritic cell expression of B7-H1 (PD-L1), a strong inhibitor of autologous T-cell activation: relevance for the immune modulatory effect in multiple sclerosis. J Neuroimmunol 155: 172–182. [PubMed: 15342209]
38. Staples KJ, Nicholas B, McKendry RT, Spalluto CM, Wallington JC, Bragg CW, Robinson EC, Martin K, Djukanovic R, and Wilkinson TM. 2015 Viral infection of human lung macrophages increases PDL1 expression via IFNbeta. PLoS One 10: e0121527. [PubMed: 25775126]
39. Heng TS, Painter MW, and C. Immunological Genome Project. 2008 The Immunological Genome Project: networks of gene expression in immune cells. Nat Immunol 9: 1091–1094. [PubMed: 18800157]
40. Bianchi R, Teijeira A, Proulx ST, Christiansen AJ, Seidel CD, Rulicke T, Makinen T, Hagerling R, Halin C, and Detmar M. 2015 A transgenic Prox1-Cre-tdTomato reporter mouse for lymphatic vessel research. PLoS One 10: e0122976. [PubMed: 25849579]
41. Wigle JT, and Oliver G. 1999 Prox1 function is required for the development of the murine lymphatic system. Cell 98: 769–778. [PubMed: 10499794]
42. Fox JM, and Diamond MS. 2016 Immune-Mediated Protection and Pathogenesis of Chikungunya Virus. J Immunol 197: 4210–4218. [PubMed: 27864552]
43. Vandenbroek MF, Muller U, Huang S, Aguet M, and Zinkernagel RM. 1995 Antiviral Defense in Mice Lacking Both Alpha/Beta and Gamma-Interferon Receptors. Journal of Virology 69: 4792–4796. [PubMed: 7609046]
44. Matsumoto M, and Seya T. 2008 TLR3: interferon induction by double-stranded RNA including poly(I:C). Adv Drug Deliv Rev 60: 805–812. [PubMed: 18262679]

45. Urcuqui-Inchima S, Cabrera J, and Haenni AL. 2017 Interplay between dengue virus and Toll-like receptors, RIG-I/MDA5 and microRNAs: Implications for pathogenesis. Antiviral Res 147: 47–57. [PubMed: 28965915]
46. Gong AY, Zhou R, Hu G, Li X, Splinter PL, O'Hara SP, LaRusso NF, Soukup GA, Dong H, and Chen XM. 2009 MicroRNA-513 Regulates B7-H1 Translation and Is Involved in IFN- -Induced B7-H1 Expression in Cholangiocytes. The Journal of Immunology 182: 1325–1333. [PubMed: 19155478]
47. Seo SK, Seo DI, Park WS, Jung WK, Lee DS, Park SG, Choi JS, Kang MS, Choi YH, Choi I, Yu BC, and Choi IW. 2014 Attenuation of IFN-gamma-induced B7-H1 expression by 15-deoxy-delta(12,14)-prostaglandin J2 via downregulation of the Jak/STAT/IRF-1 signaling pathway. Life Sci 112: 82–89. [PubMed: 25072357]
48. Lee SJ, Jang BC, Lee SW, Yang YI, Suh SI, Park YM, Oh S, Shin JG, Yao S, Chen L, and Choi IH. 2006 Interferon regulatory factor-1 is prerequisite to the constitutive expression and IFN-gamma-induced upregulation of B7-H1 (CD274). FEBS Lett 580: 755–762. [PubMed: 16413538]
49. Lee SK, Seo SH, Kim BS, Kim CD, Lee JH, Kang JS, Maeng PJ, and Lim JS. 2005 IFN-gamma regulates the expression of B7-H1 in dermal fibroblast cells. J Dermatol Sci 40: 95–103. [PubMed: 16085391]
50. Ahonen CL, Doxsee CL, McGurran SM, Riter TR, Wade WF, Barth RJ, Vasilakos JP, Noelle RJ, and Kedl RM. 2004 Combined TLR and CD40 triggering induces potent CD8+ T cell expansion with variable dependence on type I IFN. J Exp Med 199: 775–784. [PubMed: 15007094]
51. Kedl RM, and Tamburini BA. 2015 Antigen archiving by lymph node stroma: A novel function for the lymphatic endothelium. Eur J Immunol 45: 2721–2729. [PubMed: 26278423]
52. Bikfalvi A 2004 Platelet factor 4: An inhibitor of angiogenesis. Seminars in Thrombosis and Hemostasis 30: 379–385. [PubMed: 15282661]
53. Perollet C, Han ZC, Savona C, Caen JP, and Bikfalvi A. 1998 Platelet factor 4 modulates fibroblast growth factor 2 (FGF-2) activity and inhibits FGF-2 dimerization. Blood 91: 3289–3299. [PubMed: 9558385]
54. Bikfalvi A 2004 Recent developments in the inhibition of angiogenesis: examples from studies on platelet factor-4 and the VEGF/VEGFR system. Biochem Pharmacol 68: 1017–1021. [PubMed: 15313395]
55. Li S, Nie EH, Yin Y, Benowitz LI, Tung S, Vinters HV, Bahjat FR, Stenzel-Poore MP, Kawaguchi R, Coppola G, and Carmichael ST. 2015 GDF10 is a signal for axonal sprouting and functional recovery after stroke. Nat Neurosci 18: 1737–1745. [PubMed: 26502261]
56. Malan D, Wenzel D, Schmidt A, Geisen C, Raible A, Bolck B, Fleischmann BK, and Bloch W. 2010 Endothelial beta1 integrins regulate sprouting and network formation during vascular development. Development 137: 993–1002. [PubMed: 20179098]
57. Tanjore H, Zeisberg EM, Gerami-Naini B, and Kalluri R. 2008 Beta1 integrin expression on endothelial cells is required for angiogenesis but not for vasculogenesis. Dev Dyn 237: 75–82. [PubMed: 18058911]
58. Pietras EM, Lakshminarasimhan R, Techner JM, Fong S, Flach J, Binnewies M, and Passegue E. 2014 Re-entry into quiescence protects hematopoietic stem cells from the killing effect of chronic exposure to type I interferons. J Exp Med 211: 245–262. [PubMed: 24493802]
59. Tewalt EF, Cohen JN, Rouhani SJ, Guidi CJ, Qiao H, Fahl SP, Conaway MR, Bender TP, Tung KS, Vella AT, Adler AJ, Chen L, and Engelhard VH. 2012 Lymphatic endothelial cells induce tolerance via PD-L1 and lack of costimulation leading to high-level PD-1 expression on CD8 T cells. Blood 120: 4772–4782. [PubMed: 22993390]
60. Wetterholm E, Linders J, Merza M, Regner S, and Thorlacius H. 2016 Platelet-derived CXCL4 regulates neutrophil infiltration and tissue damage in severe acute pancreatitis. Transl Res 176: 105–118. [PubMed: 27183218]
61. Tan KW, Chong SZ, Wong FH, Evrard M, Tan SM, Keeble J, Kemeny DM, Ng LG, Abastado JP, and Angeli V. 2013 Neutrophils contribute to inflammatory lymphangiogenesis by increasing VEGF-A bioavailability and secreting VEGF-D. Blood 122: 3666–3677. [PubMed: 24113869]

62. Hallam DM, and Maroun LE. 1998 Anti-gamma interferon can prevent the premature death of trisomy 16 mouse cortical neurons in culture. Neuroscience Letters 252: 17–20. [PubMed: 9756348]

63. Lee HC, Tan KL, Cheah PS, and Ling KH. 2016 Potential Role of JAK-STAT Signaling Pathway in the Neurogenic-to-Gliogenic Shift in Down Syndrome Brain. Neural Plast 2016: 7434191. [PubMed: 26881131]

64. Ling KH, Hewitt CA, Tan KL, Cheah PS, Vidyadaran S, Lai MI, Lee HC, Simpson K, Hyde L, Pritchard MA, Smyth GK, Thomas T, and Scott HS. 2014 Functional transcriptome analysis of the postnatal brain of the Ts1Cje mouse model for Down syndrome reveals global disruption of interferon-related molecular networks. BMC Genomics 15: 624. [PubMed: 25052193]

65. Maroun LE 1979 Interferon effect on ribosomal ribonucleic acid related to chromosome 21 ploidy. Biochem J 179: 221–225. [PubMed: 475756]

66. Maroun LE 1996 Interferon action and chromosome 21 trisomy (Down syndrome): 15 years later. J Theor Biol 181: 41–46. [PubMed: 8796190]

67. Maroun LE, Heffernan TN, and Hallam DM. 2000 Partial IFN-alpha/beta and IFN-gamma receptor knockout trisomy 16 mouse fetuses show improved growth and cultured neuron viability. Journal of Interferon and Cytokine Research 20: 197–203. [PubMed: 10714556]

68. Tan YH, Schneider EL, Tischfield J, Epstein CJ, and Ruddle FH. 1974 Human chromosome 21 dosage: effect on the expression of the interferon induced antiviral state. Science 186: 61–63. [PubMed: 4371269]

69. Weil J, Epstein LB, and Epstein CJ. 1980 Synthesis of interferon-induced polypeptides in normal and chromosome 21-aneuploid human fibroblasts: relationship to relative sensitivities in antiviral assays. J Interferon Res 1: 111–124. [PubMed: 6180034]

70. Snell LM, McGaha TL, and Brooks DG. 2017 Type I Interferon in Chronic Virus Infection and Cancer. Trends Immunol 38: 542–557. [PubMed: 28579323]

71. Ye B, Liu X, Li X, Kong H, Tian L, and Chen Y. 2015 T-cell exhaustion in chronic hepatitis B infection: current knowledge and clinical significance. Cell Death Dis 6: e1694. [PubMed: 25789969]

72. Loo CP, Nelson NA, Lane RS, Booth JL, Loprinzi Hardin SC, Thomas A, Slifka MK, Nolz JC, and Lund AW. 2017 Lymphatic Vessels Balance Viral Dissemination and Immune Activation following Cutaneous Viral Infection. Cell Rep 20: 3176–3187. [PubMed: 28954233]

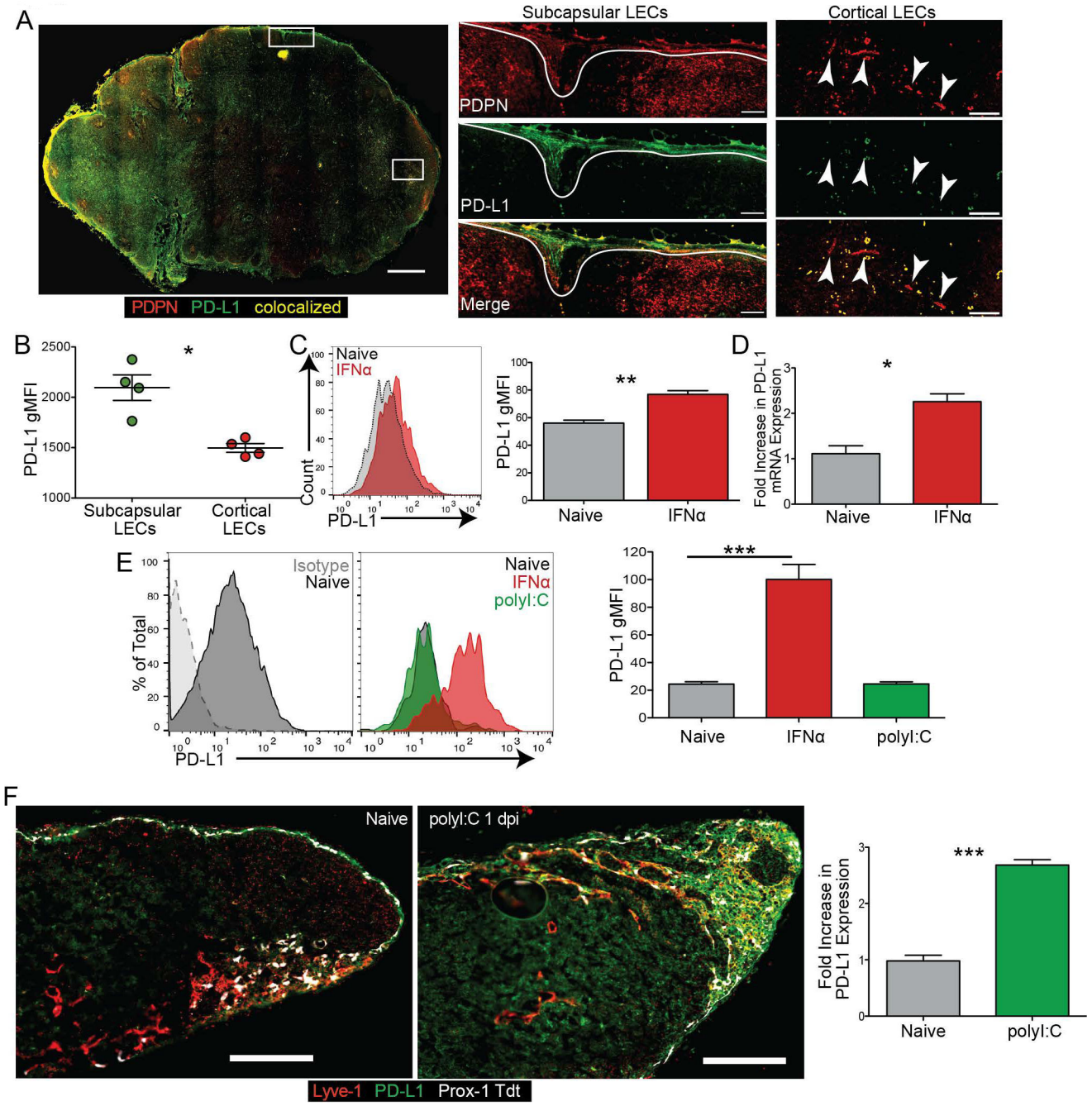

Figure 1. LEC PD-L1 expression is increased by IFNα *in vitro*.

(A) Representative image and quantification of a human normal LN stained for PDPN and PD-L1. Magnification: 200x. Arrows point to cortical lymphatic vessels. Gates were drawn on the subcapsular and cortical LECs, and the gMFI of PD-L1 expression was quantified. Large image magnification: 100x; small image magnification: 200x. Scale bar on large image: 1mm; scale bars on inset images: 100μm. (B) Quantification of A. (C) Representative plot and quantified data showing the regulation of hLEC PD-L1 expression by IFNα *in vitro*. Cells were treated with IFNα for 24 hours prior to harvest. (D) RT-qPCR of PD-L1 from hLECs treated with IFNα *in vitro*. Cells were treated with IFNα for 24 hours prior to

harvest. (E) Representative plot and quantified data showing the regulation of mLEC PD-L1 expression by IFNα and polyI:C *in vitro*. Cells were treated with IFNα or poly I:C for 24 hours prior to harvest. (F) Representative image and quantification of Prox-1 tdt murine popliteal LN from naïve and 1day post immunization with polyI:C stained for lyve-1 and PD-L1. Magnification: 200x. Scale bars: 250μm. Gates were drawn on the lyve-1 positive vessels, and the fold increase of PD-L1 expression compared to naïve was quantified. All experiments were repeated twice with 3–5 replicates per group with similar results. Statistical analysis was done using a paired or unpaired *t*-test. **, $p < 0.01$; ***, $p < 0.001$.

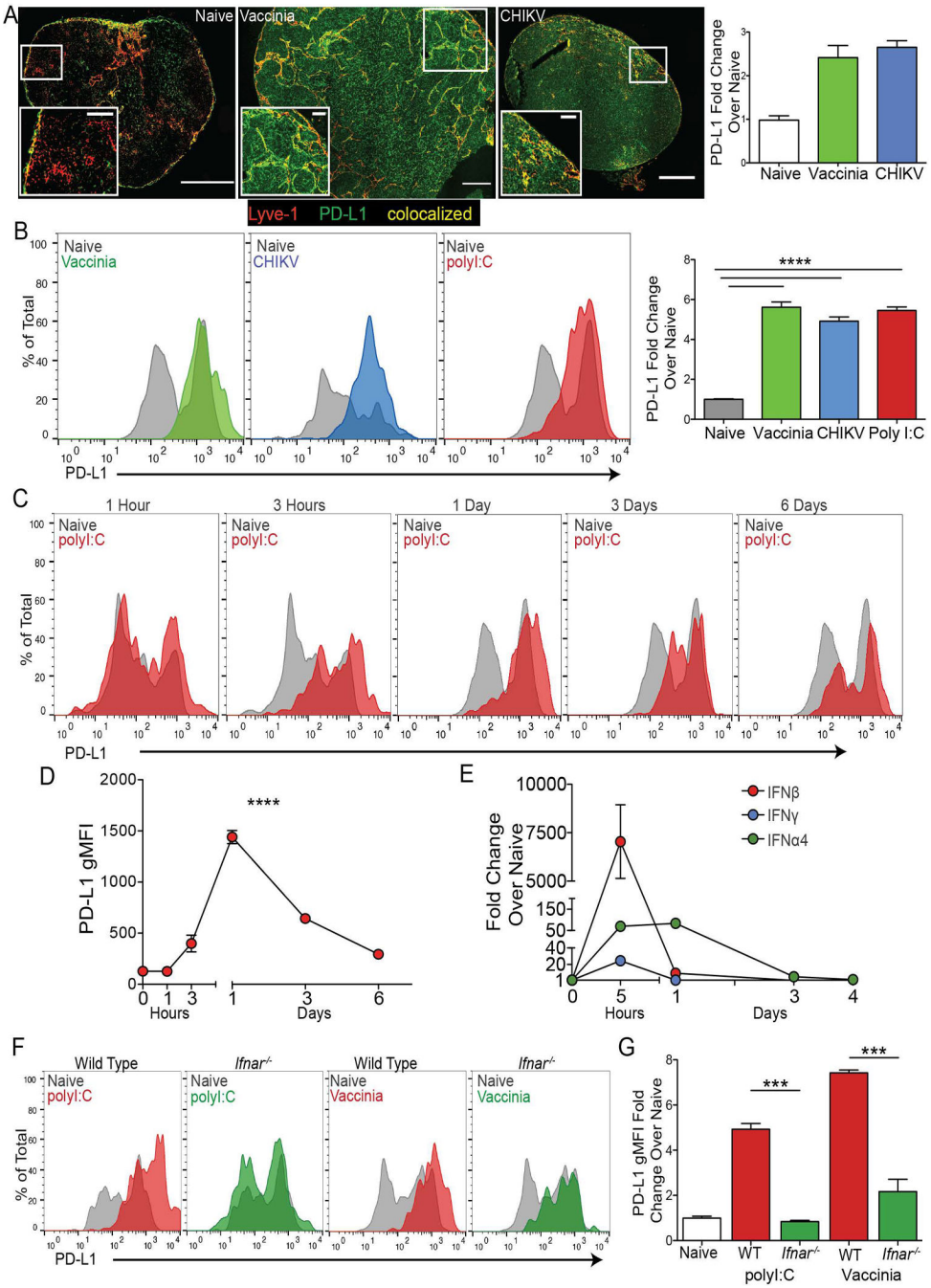

Figure 2. PD-L1 is upregulated following type 1 IFN stimulus.

(A) Representative 200x images and quantification of LNs from naïve and day 3–5 vaccinia virus and CHIKV infected mice. Sections were stained for Lyve-1 and PD-L1. Fold increase in PD-L1 expression over naïve is shown. Gates were drawn around the Lyve-1 positive staining, and the average PD-L1 gMFI was taken and normalized to naïve. Large image scale bars: 250μM; inset image scale bars: 50μM. (B) Representative plots and quantification of PD-L1 expression on LECs in the dLN following infection with vaccinia and CHIKV virus and immunization with poly I:C. The fold increase in PD-L1 gMFI compared to naïve

is shown. (C) Representative flow plots of PD-L1 expression on the dLN LECs following poly I:C immunization. (D) Quantification of C showing PD-L1 gMFI on all dLN LECs over time. (E) RT-qPCR showing fold increase in IFNα4, IFNβ and IFNγ expression in the dLN 5h post immunization with poly I:C. Data is normalized to naïve. (F) Representative flow plots and quantification of PD-L1 expression in WT and *Ifnar*$^{-/-}$ mice, 24 hours post immunization with poly I:C or 5 days post infection with vaccinia virus. The fold increase in PD-L1 expression on LECs over naïve is shown. All experiments used 2–3 replicates per group and were repeated twice with similar results. Statistical analysis was done using an unpaired *t*-test or one-way ANOVA. *, $p < 0.05$; **, $p < 0.01$; ****, $p < 0.0001$.

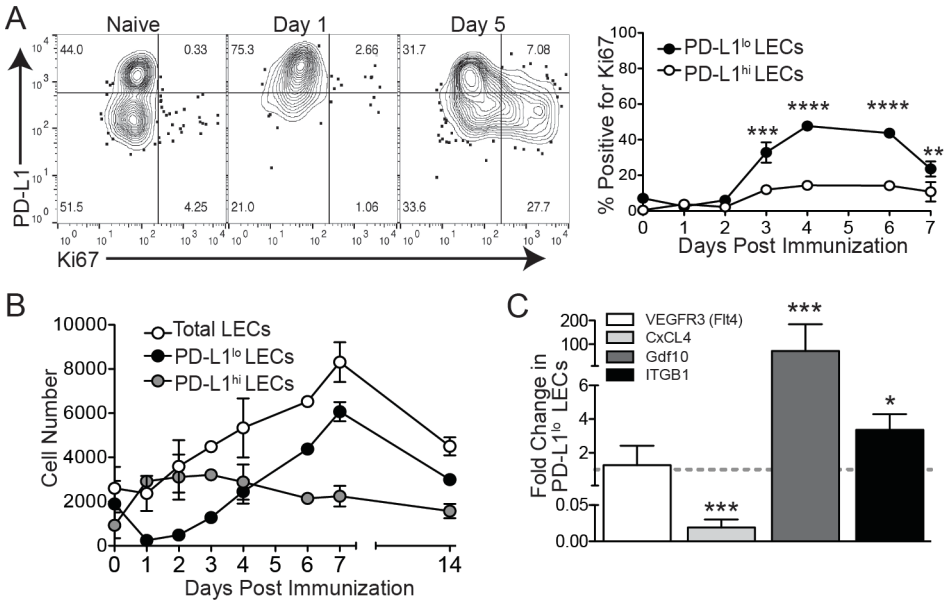

Figure 3. Only PD-L1^{lo} LECs divide in response to an interferon stimulus.

(A) Representative flow plots and quantification of PD-L1 and Ki67 expression on LECs following immunization with poly I:C and α-CD40. The percent of PD-L1^{lo} and PD-L1^{hi} LECs that are Ki67 positive is shown. (B) LEC numbers following immunization with poly I:C and α-CD40. Total LEC, PD-L1^{lo} LEC and PD-L1^{hi} LEC number is shown. (C) RT-qPCR showing the expression fold change in PD-L1^{lo} LECs 6 days post immunization. All experiments used 2–3 replicates per group and were repeated twice with similar results. Statistical analysis was done using a one-way ANOVA. ****, $p < 0.0001$.

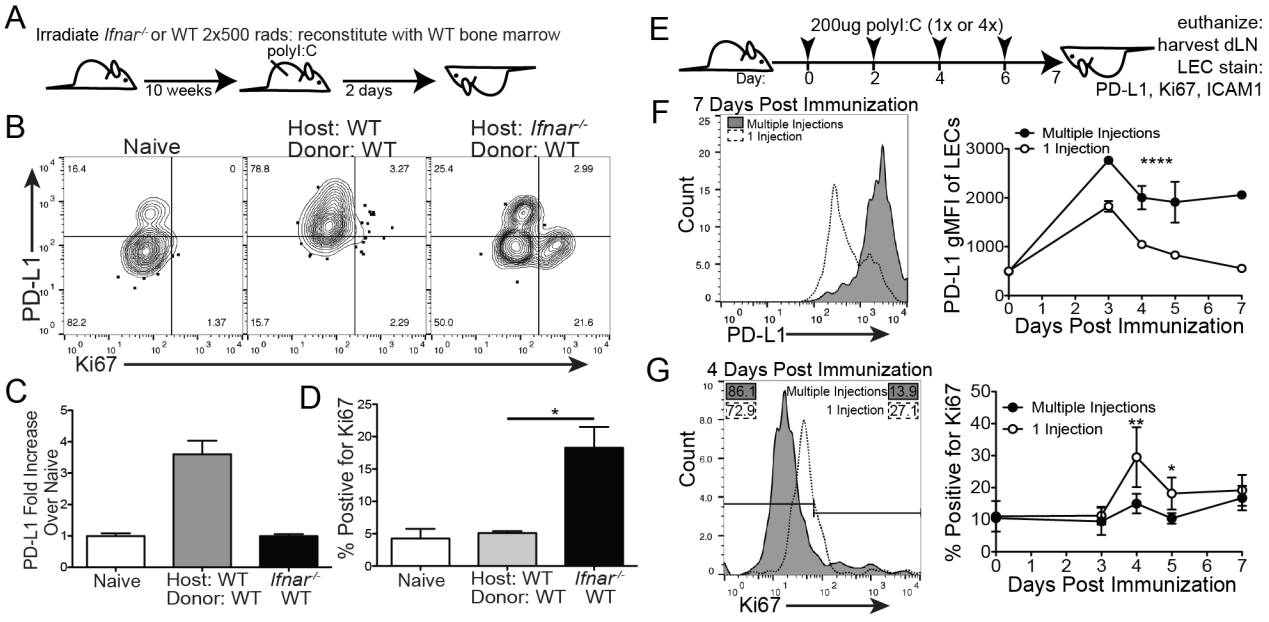

Figure 4. Type 1 IFN inhibits LEC division and promotes PD-L1 upregulation.

(A) Schematic of experimental design for B-D. (B) Representative flow plots showing PD-L1 and Ki67 in WT and *Ifnar*$^{-/-}$ chimeras 2 days post immunization. (C) Quantification of A showing PD-L1 expression on LECs. (D) Quantification of A showing the percent of total LECs that are Ki67 positive. (E) Schematic of experimental design for F-G. (F) Representative flow plots and quantification showing PD-L1 expression on LECs 7 days post immunization. (G) Representative flow plots and quantification displaying Ki67 expression on LECs 4 days post immunization. All experiments used 3 replicates per group and were repeated twice with similar results. Statistical analysis was done using an unpaired *t*-test or one-way ANOVA. *, $p < 0.05$; **, $p < 0.01$; ****, $p < 0.0001$.

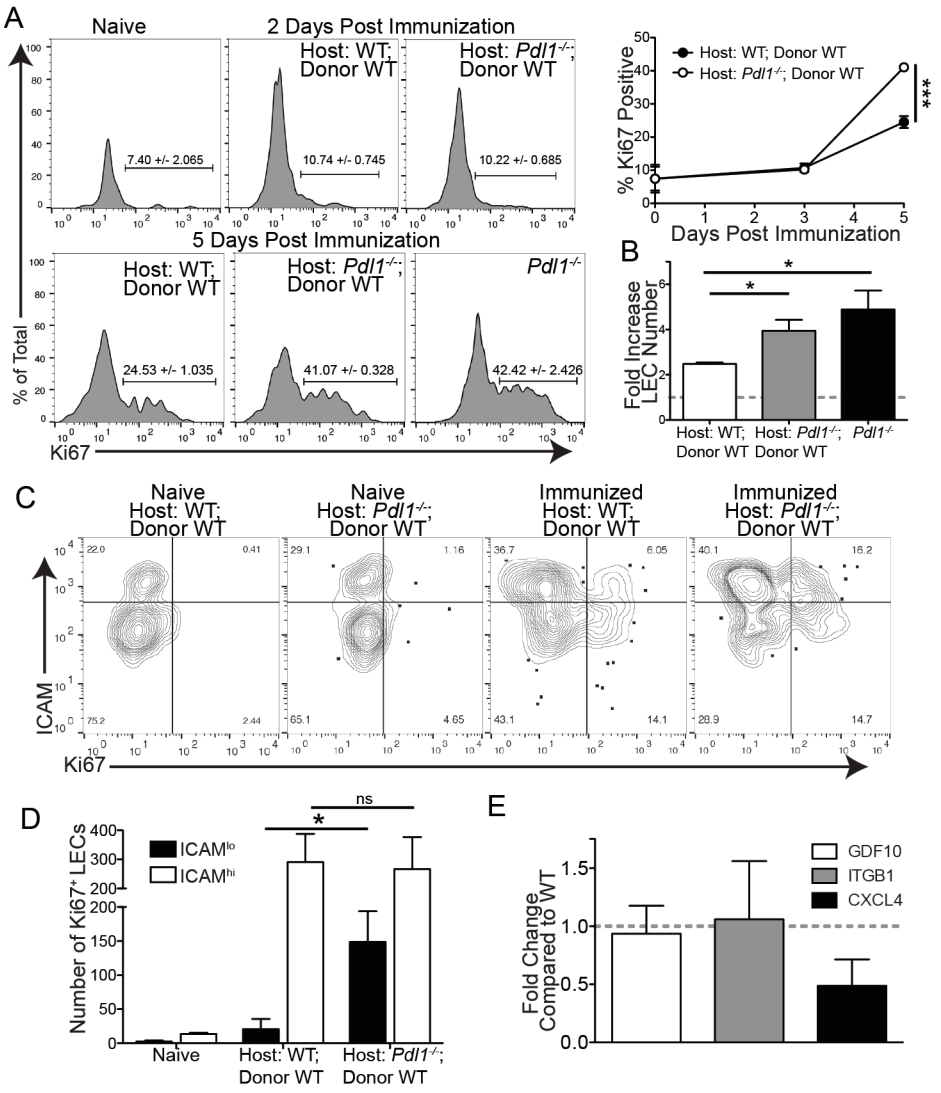

Figure 5. Loss of PD-L1 promotes LEC division after immunization.

(A) Representative flow plots and quantification showing Ki67 expression in WT and *Pdl1*$^{-/-}$ chimeras, and the total *Pdl1*$^{-/-}$ 2 and 5 days post immunization. Day 5 WT compared to Day 5 *Pdl1*$^{-/-}$ chimeras: p = 0.0001; Day 5 WT compared to total Day 5 *Pdl1*$^{-/-}$: p = 0.008. (B) The fold increase in total LEC number over naïve. (C) Representative flow plots displaying Ki67 expression by ICAM1 expression in WT and *Pdl1*$^{-/-}$ chimeras. (D) Quantification of C showing the number of Ki67^{+}, ICAM1^{hi} LECs. (E) RT-qPCR showing the expression fold change in *Pdl1*$^{-/-}$ LECs 6 days post immunization. All experiments used 3 replicates per group and were repeated twice with similar results. Statistical analysis was done using a one-way ANOVA following by Bonferroni's post-test. *, $p < 0.05$.

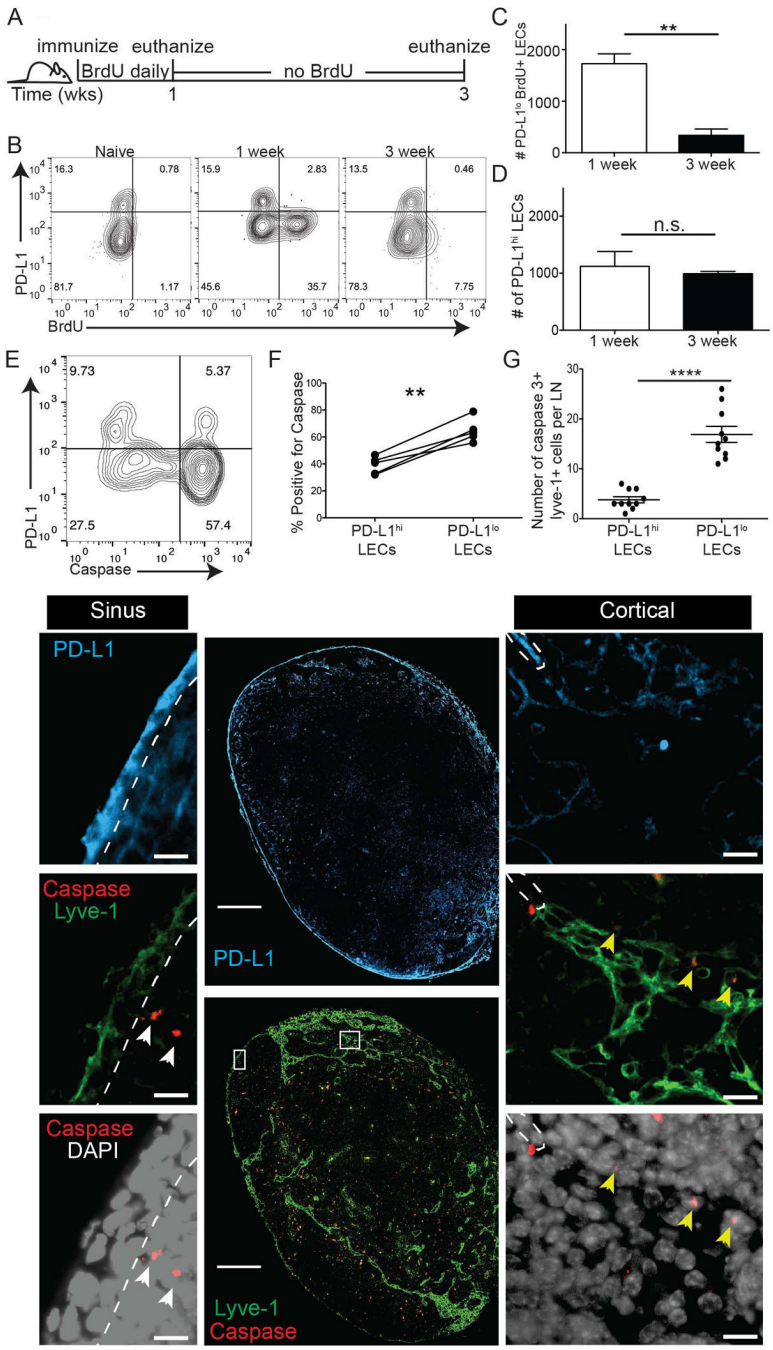

Figure 6. PD-L1^{+} LECs are protected from apoptosis.

(A) Schematic of experimental design for B-D. (B) Representative flow plots showing PD-L1 expression and BrdU incorporation on LECs. (C) Quantification of B showing the number of BrdU^{+} PD-L1^{lo} LECs. (D) Quantification of B showing the number of PD-L1^{hi} LECs. (E) Representative flow plot displaying PD-L1 and cleaved caspase 3,7 expression on LECs. (F) Quantification of (E) displaying the percent of PD-L1^{lo} and PD-L1^{hi} LECs that are cleaved caspase 3,7 positive. (G) Quantification and representative images of an inguinal LN stained with lyve-1, PD-L1, cleaved caspase 3 and DAPI. Magnification on large image:

20x; magnification on inset images: 40x. Scale bars on large images: 250μm; scale bars on inset images: 10μm. Quantification displays the number of cleaved caspase 3 positive PD-L1^{+} and PD-L1^{-}LECs per LN section. All experiments used 3 replicates per group. BrdU staining was repeated 4 times, caspase flow staining was repeated twice and caspase IF was repeated 4 times with 4 lymph nodes per group with similar results. Statistical analysis was done using a paired or unpaired *t*-test. **, $p < 0.01$; ****, $P < 0.0001$.

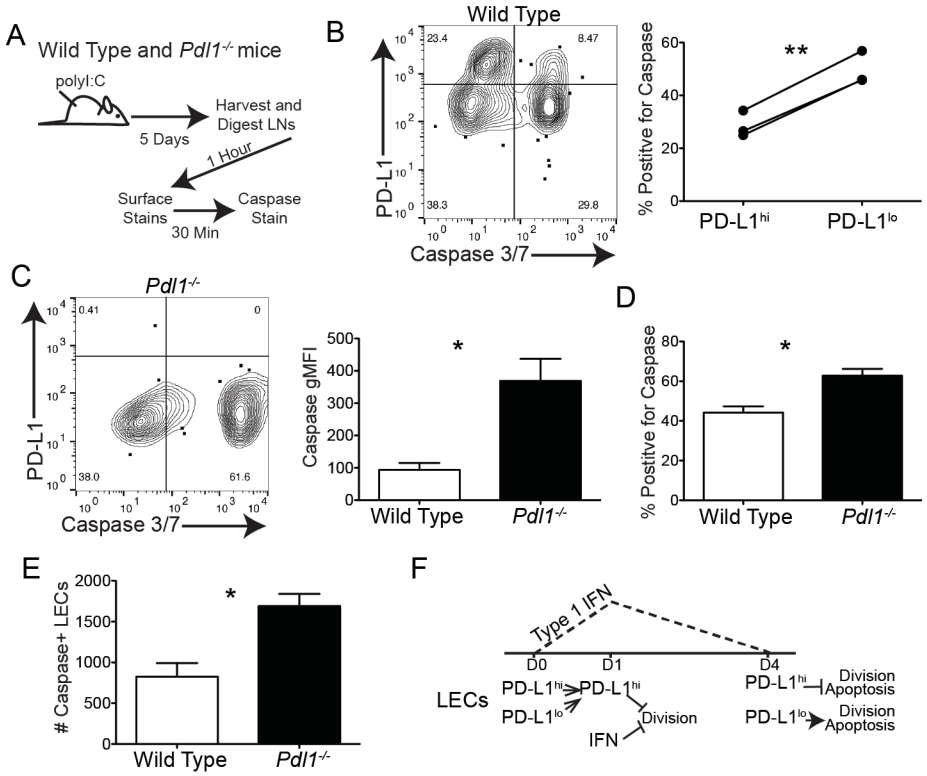

Figure 7. Loss of PD-L1 increases LEC apoptosis following immunization.

(A) Schematic of experiment design for Figure B-E. (B) Representative flow plot and quantification of caspase3/7 staining on WT LECs 5 dpi. (C) Representative flow plot and gMFI quantification of caspase3/7 staining on WT and *Pdl1*$^{-/-}$ LECs 5 dpi. (D) Quantification displaying percent of LECs positive for caspase 3/7 expression in WT and *Pdl1*$^{-/-}$ LECs 5 dpi. (E) Quantification displaying of number of caspase 3/7 positive LECs expression in WT and *Pdl1*$^{-/-}$ LECs 5 dpi. (F) Model of type 1 IFN and PD-L1 regulation of division and survival of LECs. All experiments used 3 replicates per group and were repeated twice with similar results. Statistical analysis was done using a one-way ANOVA following by Bonferroni's post-test. *, $p < 0.05$.